



Research papers

Low-flow behavior of alpine catchments with varying quaternary cover under current and future climatic conditions



Marie Arnoux^{a,e,*}, Philip Brunner^a, Bettina Schaefli^{b,c}, Rebecca Mott^d, Fabien Cochand^a, Daniel Hunkeler^a

^a Université de Neuchâtel, Centre d'Hydrogéologie et de Géothermie (CHYN), Rue Emile Argand 11, 2000 Neuchâtel, Switzerland

^b Institute of Earth Surface Dynamics, University of Lausanne, Géopolis Building UNIL Mouline, 1015 Lausanne, Switzerland

^c Institute of Geography, University of Bern, Hallerstrasse 12, 3012 Bern, Switzerland

^d WSL Institute for Snow and Avalanche Research SLF, Flüelastrasse 11, 7260 Davos Dorf, Switzerland

^e Centre de recherche sur l'environnement alpin (CREALP), Rue de l'Industrie 45, 1951 Sion, Switzerland

ARTICLE INFO

This manuscript was handled by Marco Borga, Editor-in-Chief, with the assistance of Michael Bruen, Associate Editor

Keywords:
Hydrology
Alpine catchments
Groundwater storage
Snow
Climate change

ABSTRACT

Alpine environments are particularly vulnerable to climatic warming, and long term observations suggest a shift of snow-influenced river discharge towards earlier periods of the year. For water resources management, the seasonal patterns of discharge in alpine areas are particularly relevant, as the shift to lower flows in summer and autumn combined with increased water demand could lead to water shortage in downstream catchments. The storage of groundwater in alpine catchments could significantly modulate how changing climatic conditions influence the annual streamflow regime. However, groundwater storage and its buffering capacity in alpine areas remain poorly understood. Moreover, studies on how climate change will impact water resources in alpine areas rarely consider the influence of geology.

In this paper, catchment geology is used as a basis for the classification of future summer low flows behavior of several alpine catchments in Switzerland. Based on the analysis of the relationship between low-flow indicators and geology, the role of unconsolidated quaternary deposits is explored. We show that quaternary deposits play a critical role in the seasonal storage of groundwater, which can contribute to rivers during low-flow periods. Three climate change simulations based on extreme RCP 8.5 scenarios are fed into a conceptual hydrological model to illustrate the buffering role of groundwater. Past and future low flows normalized by mean past and future streamflows appear correlated with the percentage of unconsolidated quaternary deposits. These results highlight that catchments with high groundwater contribution to streamflow relative to precipitation will have a slower decrease in future summer discharge. Therefore, we propose two indicators that can be used to anticipate the response of future summers low flows in alpine areas to climate change: the current winter low flows and the percentage of unconsolidated quaternary deposits of the catchments.

1. Introduction

Alpine areas greatly affect streamflow dynamics through their seasonal storage of water. They are defined as mountainous regions with steep slopes, snowmelt dominated, located mostly above the tree line, where little or no soil and vegetation are present (Hayashi, 2020). During winter, water is stored in the form of snow before being released during warmer periods by melt processes, thus controlling the seasonal hydrograph (Freudiger et al., 2017). This seasonal redistribution of water can significantly reduce the consequences of meteorological droughts in lowlands during summer (Beniston and Stoffel, 2014;

Rohrer et al., 2013); however, alpine areas are also highly sensitive to climate change.

Climate change and the associated increasing temperatures result in shorter snow cover durations. More precipitation is, therefore, falling as rain than as snow during the winter period (Harpold and Brooks, 2018; Li et al., 2017; Zhang et al., 2015). These changes in snowfall fraction will also lead to a decrease in seasonal snow accumulation which can be accentuated by more mid-winter melt events (Cochand et al., 2019a; Pavlovskii et al., 2019). Consequently, winter low flows, typical for alpine catchments, are expected to become less extreme in magnitude (Laaha et al., 2016). Moreover, the onset of snowmelt will be shifted

* Corresponding author at: Centre de recherche sur l'environnement alpin (CREALP), Rue de l'Industrie 45, 1951 Sion, Switzerland.

E-mail addresses: marie.arnoux@crealp.vs.ch (M. Arnoux), philip.brunner@unine.ch (P. Brunner), bettina.schaefli@giub.unibe.ch (B. Schaefli), mott@slf.ch (R. Mott), fabien.cochand@gmail.com (F. Cochand), Daniel.Hunkeler@unine.ch (D. Hunkeler).

toward earlier spring (Barnett et al., 2005; Godsey et al., 2014). These changes will lead to a lower streamflow peak occurring earlier in the year (Jenicek et al., 2018) and a decrease of spring streamflow (Barnhart et al., 2016; Teutschbein et al., 2015). These changes will probably also lead to a reduction in stream discharges in summer and autumn (Barnett et al., 2005; Berghuijs et al., 2014; Lauber et al., 2014; Musselman et al., 2017), which can considerably affect water resources management of downstream catchments. However, hydrological modelling has already shown that snowmelt alone cannot explain the variability of future summer low flows (Jenicek et al., 2016).

Elevation influences local air temperature and thus changes in snow storage. Marty et al. (2017) showed that, in the European Alps, relative SWE could potentially decrease about 50% at high elevations ($\sim 3,000$ m a.s.l.) and almost no snow might accumulate at elevations lower than 1'200 m a.s.l. by the end of the century. The largest absolute decrease in maximum annual SWE was predicted for elevations from 2'000 to 2'700 m a.s.l. (Jenicek et al., 2018).

A considerable proportion of hydrological research dedicated to alpine catchments focused on the analysis of alpine stream hydrographs with snowmelt processes during spring and early summer (Garvelmann et al., 2017; Jodar et al., 2016; Lauber et al., 2014; Staudinger et al., 2017; Zuecco et al., 2018). However, hydrological processes that pertain to the subsurface can also be highly relevant. Groundwater discharge to streams is often the principal component of the streamflow from Alpine basins during extended periods of the year, especially during winter low flows (Clow et al., 2003; Cras et al., 2007; Hood et al., 2006; Huth et al., 2004; Jodar et al., 2017; Liu et al., 2004). To date, it remains unclear to what extent groundwater stored in Alpine catchments can mitigate the potentially adverse effects of climate change (Hayashi, 2020; Vivioli et al., 2007). Thus, there is an urgent need to better understand the capacity of Alpine areas to store groundwater, as well as the associated dynamics. In a recent review paper on the main Alpine aquifers across the world, Hayashi (2020) highlighted the role of aquifers in unconsolidated deposits to explain the fast recession of discharge after the recharge period (i.e., snowmelt) or rainfall events, followed by a slower recession that sustains discharge over a long period. According to Hayashi (2020), this two-phase recession is likely controlled by groundwater system dynamics. Spencer et al. (2019) showed the importance of both fractured permeable bedrock and glacial till deposits for runoff generation in Canada's Rocky Mountains. Wirth et al. (2020) showed that Quaternary deposits are important for groundwater contribution to streamflow in the Swiss Prealps. Several recent publications highlighted the role of Quaternary deposits to store groundwater in alpine regions (Christensen et al., 2020; Arnoux et al., 2020). However, the linkage between geology, groundwater, and streamflow regime response to climate change has not previously been addressed explicitly and is the purpose of this paper.

In addition to the important practical implications of this situation concerning water resources management, the scientific understanding of hydrogeological processes in alpine areas remains in its infancy. Some studies have shown that a change in snow regime affects groundwater recharge (Tague and Grant, 2009) and thus impacts streamflow (Godsey et al., 2014). In snow-dominated areas, the main recharge period occurs during the melt period and there is little recharge during the winter period. The total amount of snow precipitation in winter affects groundwater recharge and hence streamflow during dry summer periods (Beaulieu et al., 2012; Van Loon et al., 2015). However, the link between groundwater storage and streamflow regime changes is difficult to determine.

In this context, the main objectives of this study are: (1) to determine if and how current low-flow rates are related to the geology of alpine catchments; (2) to discuss the consequences of climate change for future winter and summer low flows and evaluate the influence of dynamic groundwater storage on flow rates; (3) to establish the link between geology and catchment response to climate change. For this

purpose, we have selected 13 catchments across the Swiss Alps. We first compared their low-flow characteristics with the surface geology to classify them. Subsequently, past and future streamflow dynamics were simulated using the conceptual hydrological HBV model (Seibert, 2000). We focused on groundwater contribution to streamflows and its impact on summer low flows. To better represent the streamflow and groundwater dynamics, we consider the seasonal and inter-annual variability in streamflow and groundwater storage by running three of the latest simulations of the extreme RCP8.5 CH2018 climate change scenario, continuously from the past (starting 1981) until the end of this century (ending 2099).

2. Study sites

Thirteen gauged Alpine catchments were selected across the Swiss Alps. Their surface areas range from 8.1 to 55.3 km², allowing a relation between groundwater storage and specific catchment characteristics. Their mean elevations range from 1'702 to 2'567 m asl, high enough to be considered as Alpine catchments but also without - or only very small - areas covered by glaciers. They were also selected as they are nearly undisturbed by man-made infrastructure (dams, pumping, etc.). Three exceptions can be indicated: catchment #1, for which a known volume of water is pumped for drinking water, and #4 and #5, which can have various minor influences (i.e. low volume of pumping or water transfer).

The location of the chosen catchments is illustrated in Fig. 1 and their main characteristics are described in Table 1. Fig. 2 illustrates the distribution of elevation versus slopes. These catchments are all snowmelt dominated with a snow cover period of a few months, a snow accumulation period between 5 and 7 months, and a snowmelt period of 2 to 3 months (based on 2016–2018 snow data, see part 3.1 for the description of snow data). Catchments with the strongest snow accumulation are #6, #2, #9, #1, and the ones with the lowest accumulation rates are #10 and #8.

Catchment #1 has been monitored for a few years and its hydrogeology has already been studied (see Cochand et al. (2019b) for more details). Catchments #3 to #13 are part of the Swiss hydrological network (HUG) and some of them have been considered in previous studies focusing on future climate impacts or low-flows analyses (Addor et al., 2014; Jenicek et al., 2018, 2016; Staudinger and Seibert, 2014; Staudinger et al., 2017, 2015) but without specifically focusing on the role of groundwater and geology in catchment dynamics, which is the purpose of this paper.

The geology of the catchments has been extracted from the surface geological maps (1:25'000) from Swisstopo (2018). In this paper, we focus on the role of deposits common for each catchment, which are the Quaternary deposits. These deposits are mainly talus, moraine, alluvium or cones. The permeability of Quaternary deposits can be variable but the rocks are characterized by relatively high porosity and permeability. For example, in the Canadian Rockies, Muir et al. (2011) observed that talus has a very high hydraulic conductivity (0.01 to 0.03 m/s) and limited storage capacity with sometimes a residence time-scale of less than a week. Conversely, moraines have been regularly observed to have lower hydraulic conductivities in the approximate ranges of 10^{-6} to 10^{-4} m/s for lateral moraines and 10^{-5} to 10^{-4} m/s for frontal moraines (Vincent et al., 2019). They are mostly composed of clays, silts, sands and gravels, where the sands and gravels can be many orders of magnitude higher in permeability compared to the fractured crystalline rocks.

There is no information available on the depths of these deposits for the study catchment except catchment #12 and #1. For catchment #12, the estimated average is in the range of 0.5–10 m (Florianic et al., 2018). For catchment #1, a geophysical study has estimated alluvium sediment to be at a maximum 38 m depth in the valley bottom (Geotest, 1963). In the literature, the thickness of Quaternary sediments has been estimated to be up to 30–40 m in the meadow (Christensen et al., 2020).

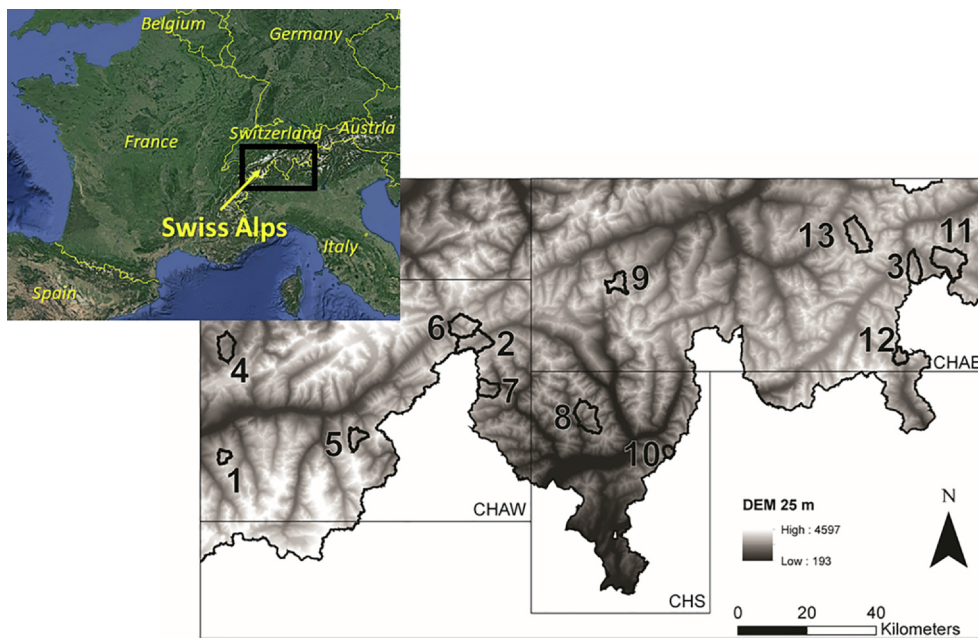


Fig. 1. Study site location, the climate areas CHAW, CHS and CHAE are represented around the study catchments; for the exact areas, see CH2018 (2018a).

The thickness of the moraine has been estimated to be up to 16–30 m in the Canadian Rockies (Langston et al., 2011). Hayashi (2020) acknowledge that the total thickness of alpine sediments such as talus may not be the controlling parameter of groundwater storage but rather the bedrock topography underneath the deposits. As the depth of Quaternary sediments is not available for all studied catchments, the percentage of Quaternary cover (the surface of Quaternary deposits divided by the catchment surface) is used as a metric to compare low-flows indicators to this specific type of geology.

3. Methods

The alpine catchments are firstly classified based on their geology and on their capacity to store water, derived from a set of low-flow indicators (Section 3.4). Then, based on historical data, the discharges are simulated with a conceptual hydrological model which is calibrated to fit historical streamflow data with a focus on winter low flows (Section 3.3). Finally, we apply climate change projections (Section 3.2) to the calibrated models to determine the role of groundwater in buffering future streamflow regime changes.

3.1. Data collection and processing

Daily gridded precipitation and 2 m high air temperature data (2 km resolution) from 1961 to 2018 are provided by the Swiss Federal Office of Meteorology and Climatology (CH2018, 2018a). An area-averaged time series of precipitation and air temperature is obtained for each catchment by averaging at each time step the values of all grid cells normalized by the area of the cells contained in the catchment (between 2 and 11 grid cells per catchment).

Daily discharge data were obtained from gauging stations monitored by the Swiss Federal Office for the Environment (OFEV; catchments #3 to #13), by the canton of Ticino (#2) and by the University of Neuchâtel (#1). The availability period of the monitored streamflow data for each catchment is summarised in Table 1. Based on the analysis of the geology underlying the gauging stations, we assume that groundwater flowing below gauging stations (i.e. bypassing them) is negligible (Table 1).

Mean daily snow water equivalent (SWE) data were available for three years and for each catchment (period 01.09.2015–31.08.2018).

These data were based on daily snow depth observations from over 300 Swiss snow monitoring stations. The observations were assimilated into a physically-based snowpack model run at 250 m spatial and hourly temporal resolution, which were then upscaled to one average SWE value per catchment and per day. Details about monitoring data, snowpack modeling, and data assimilation methods are available from Griessinger et al. (2019) and Winstral et al. (2019). These daily mean SWE data are used here to calibrate the snow routine of the HBV model (see Section 3.3.3).

The dominant geology per catchment is derived from the Swiss geological map 1:25'000 (SwissTopo, 2018). Topographic watershed and slopes are obtained using the Digital elevation model at 25 m (SwissTopo, 2008) on ArcGIS software 10.4.1.

3.2. Climate projections

The recent Swiss Climate Change Scenarios 2018 data set (CH2018, 2018a) is used to simulate the impact of future changes in air temperature and precipitation on dynamic groundwater storage in alpine catchments and its influence on stream discharge. The CH2018 data set is based on global climate modeling combined with downscaling using regional climate models and quantile mapping (CH2018, 2018b). The data set consists of daily gridded air temperature and precipitation from 1981 to 2099 at a resolution of 2 km. Catchment-average time series of daily precipitation and air temperature are obtained by averaging all grid cells normalized by the area of the cells contained in the catchment (between 2 and 11 grid cells per catchment).

It is important to note that the climate data may not replicate the reality because of the difficulty in accurately determining temperature and precipitation in highly heterogeneous environments such as Alpine areas. Besides, a resolution of 2 km is higher than what would be necessary for the size of our study catchments. These sources of uncertainty are acceptable for our study as the aim is to determine the sensitivity of the catchments to changes. Also, focusing our analysis on relative differences between a reference period and future climate change impact simulations reduces the uncertainty linked to systematic biases.

Following the recommendations of the CH2018 report (CH2018, 2018a), 30-year means are compared. A reference period (Ref: 1982–2011) is compared to three future periods (2035: 2020–2049,

Table 1

Catchments characteristics; geological information is based on the geological map 1:250000 ([Swisstopo, 2018](#)). Glacier cover has been estimated in 2015 ([OFEV, 2020](#)) and has decreased by now. Mean discharge (Q) is calculated from daily discharge measurements on the monitoring periods. Mean precipitation (P) is obtained RhinesD product ([MeteoSuisse, 2019](#)) data and mean potential evapotranspiration (ETP) is calculated from Oudin's formula ([Oudin et al., 2005](#), 2005) from temperature of TabsD data ([MeteoSuisse, 2019](#)), on the period 1961–2018.

Number	Name	Streamflow monitoring periods	Q (mm/yr)	Surface of topographic catchment (km ²)	Mean elevation (m asl)	Minimum elevation (m asl)	Maximum elevation (m asl)	Geology under gaging station	Glacier cover (%)	P (mm/yr)	ETP (mm/yr)
#1	Réhy	2013–2018	946	10.5	2567	2100	3100	28	Gneiss	0.0	976
#2	Station 10	1990–2018	968	43.3	2267	1466	3051	40	Alluvium	0.9	1930
#3	Ova da Cluozza	1961–2018	908	27.0	2368	1509	3165	51	Gneiss	0.0	917
#4	Allenbach	1960–2018	1337	28.8	1863	1297	2762	38	Clay/ Sandstone/ Limestone	0.0	1593
#5	Krummbach	1960–2018	1243	19.8	2276	1795	3268	35	Gneiss	0.4	1380
#6	Goneri	1990–2018	2008	38.5	2383	1395	3192	45	Moraine	4.0	1985
#7	Riale di Calleggia	1967–2018	1841	23.9	1996	890	2921	55	Gneiss	0.0	1860
#8	Riale di Pincasia	1992–2018	2061	44.5	1705	536	2521	57	Gneiss	0.0	1988
#9	Rein da Sunvitg	1960–1974 & 1977–2018	2152	21.8	2450	1490	3168	41	Granite	1.7	1537
#10	Riale di Roggasca	1966–2018	1990	8.1	1702	981	2316	46	Gneiss	0.0	1698
#11	Ova dal Fuorn	1960–2018	594	55.3	2327	1699	3168	36	Dolomite	0.0	910
#12	Poschiavino - La Rosa	1970–2018	1237	14.1	2283	1860	3032	37	Gneiss	0.0	1447
#13	Dischimbach	1963–2018	1239	43.2	2372	1668	3146	41	Gneiss	0.7	978
											356

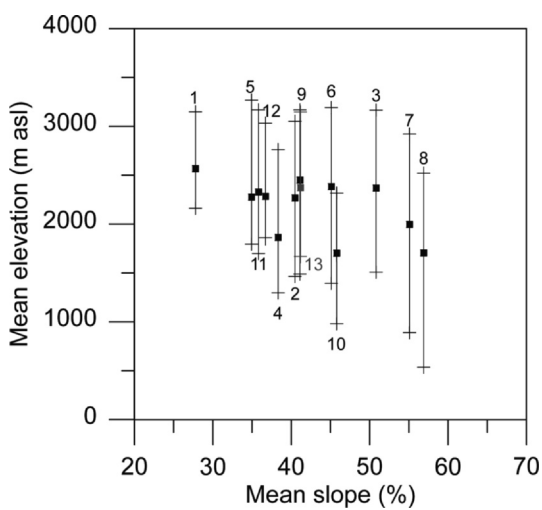


Fig. 2. Slope and range of elevations; the dots indicate the mean elevation and the numbers represent the study catchments (see [Table 1](#)).

2060: 2045–2074, and 2085: 2070–2099). Three climate change model-chains are selected because of their spring temperature evolutions in the two regions CHAW and CHAE, where most of the study catchments are located ([Fig. 1](#)).

We selected RCP 8.5 scenarios to cover the greatest impact on the hydrological cycle. In addition, we selected projections with a strong increase in spring temperature to explicitly study the effect of groundwater on future summer low flows. High spring temperature affects snowmelt the most and therefore groundwater recharge during the snowmelt period. The three chosen model chains have also different seasonal evolutions of precipitation, as summarized in [Table 2](#). Scenario S1 has the highest increase in spring temperature, S3 follows a high increase in winter and spring temperature along with a strong decrease in summer precipitation, and S2 is between both, with a lower increase in winter and spring temperatures than S1 and a lower decrease in summer precipitations than S3.

3.3. Model

3.3.1. Description

The HBV model ([Bergström, 1995](#); [Lindström et al., 1997](#)) is a bucket-type model. In this study, HBV-light is used ([Seibert and Vis, 2012](#)). This model uses different model routines to simulate catchment-scale discharge based on time series of daily precipitation and air temperature as well as estimates of daily potential evapotranspiration. A detailed description of the model can be found in the work of [Bergström \(1995\)](#), [Lindström et al. \(1997\)](#) and [Seibert \(2000\)](#). The model consists of four model routines to simulate catchment runoff: (1) the snow routine: snow accumulation and melt are computed by a degree-day method, (2) the soil routine where infiltration to the upper groundwater box and actual evapotranspiration are simulated as functions of the water storage in the soil box, (3) the response routine where runoff is computed as a function of water storage in an upper (fast) and a lower (slow) groundwater reservoir, and (4) the routing routine where a triangular weighting function routes the runoff to the outlet of the catchment. Routines 2 to 4 are run here in a lumped mode for the entire catchment; the snow routine is run based on a set of elevation bands (see [Section 3.3.3](#)). The corresponding simulated snow melt is then averaged at catchment-scale and, together with liquid rainfall, fed into routines 2 to 4.

This conceptual model is based on the following assumptions: (1) there is no other inflow into the stream except flows generated by the above routines and (2) aquifers respond as linear reservoirs. The groundwater storage is the sum of water contained in the two upper and

Table 2

Description of the used CH2018 climate change scenarios, changes in seasonal mean temperature (ΔT in $^{\circ}\text{C}$) and changes in seasonal mean precipitation (ΔP in %) according to different variables/indicators for different seasons (DJF/MMA/JJA) for the regions CHAW and CHAE and RCP8.5 at the end of the century (period 2070–2099); the captions “mean, minimum and maximum” represent the ranges of variation for all the 21 model chains (CH2018, 2018a; 2018b). Season SON is not shown because this season represents less interest for this study, as explained in the text; however, the data are available in the report (CH2018, 2018a; 2018b).

GCM	RCM	RCP	ID	DJF ΔT		MAM ΔT		JJA ΔT		DJF ΔP		MAM ΔP		JJA ΔP					
						CHAW	CHAE	CHAW	CHAE	CHAW	CHAE	CHAW	CHAE	CHAW	CHAE				
				MOHC-HadGEM2-ES	SMHI-RCA4	8.5	S1	6.5	6.8	5.2	5.3	7.3	7.2	3.9	17.0	3.7	12.0	-1.6	11.0
MPI-M – MPI – ESM – LR						S2		5.2	5.4	4.0	4.3	6.0	5.9	14.0	24.0	0.3	4.8	-19.0	-3.8
CCCma-CanESM2						S3		4.3	4.6	4.9	4.8	7.8	7.5	13.0	14.0	-6.1	-5.9	-29.0	-20.0
Mean		8.5	-	4.1	4.2	3.7		3.7	5.6	5.4	10.9	14.4	1.3	5.7	-18.9	-10.2			
Minimum				3.0	3.1	2.5		2.4	3.7	3.7	-3.5	-2.7	-14.0	-11.0	-40.0	-38.0			
Maximum				6.5	6.8	5.2		5.3	7.8	7.5	23.0	24.0	28.0	28.0	3.9	16.0			

lower groundwater boxes (Li et al., 2015).

Potential evapotranspiration is calculated with Oudin's formula based on latitude and daily air temperature (Oudin et al., 2005). Actual evapotranspiration is then computed by reducing the potential evapotranspiration as a function of soil water deficit (Seibert and Vis, 2012).

The sensitivity and uncertainty of the model parameters of the HBV model have been widely studied in Sweden and Norway. Bergström (1976) mapped the mean square error function of streamflow by the trial and error method. Seibert (1997) found that the sensitivity was hard to be described quantitatively since the sensitivity changes greatly with different parameter values. For snowmelt dominated catchments, the main uncertainties come from snow parameters (mainly the threshold air temperature for snow accumulation and snowmelt and the degree-day factor) and the recession coefficients of both groundwater boxes (Li et al., 2015). Compared to the original HBV model, the version HBV-light used here has a “warming-up period”, one year is used in our case with no limitation for the routing parameter (see Seibert and Vis (2012) for detailed information).

3.3.2. Model calibration and validation

Model calibration and validation are done in three steps: (1) snow parameters are calibrated independently on the three years of available SWE data (2015–2018); (2) hydrological parameters are then calibrated on the entire period of measurements until 2015, and finally (3) the joint performance of all model parameters are validated on the last three years of measurements 2015–2018.

Simulations are run for nine catchments (#1, #3, #6, #7, #9, #10, #11, #12, #13). The four other catchments (#8, #5, #2 and #4) are not considered in the simulations. The main reasons for this choice are short time-series and lack in streamflow measurements (#2 and #8) or anthropogenic influences (such as water abstraction) on the streamflow (#4 and #5). These last four catchments are therefore not presented in the results based on simulations (see part 4.).

3.3.2.1. Snow parameters calibration. Catchments were divided into elevation zones (from 6 to 11 zones) depending on their elevation ranges (see Table 1). The elevation ranges are not used for the generation of streamflow but they allow the calibration of both precipitation and air temperature gradients. For future periods, the gradients are kept constant. These two gradients and the snow routine parameters (threshold temperature, degree-day factor, seasonal variability in degree-day factor) were first calibrated to reproduce daily SWE data (c.f. Section 3.1) from September 1, 2015, to August 31, 2018. As only one threshold parameter for snow accumulation and melt is implemented in the HBV model snow routine, it was included as part of the calibration. This first step of the calibration is conducted for each catchment using the genetic calibration algorithm (GAB) of HBV by which optimized parameter sets are found by consecutive evolution of parameter sets using selection and recombination (Seibert and Vis, 2012). The objective function for this optimization is obtained

following an integrated multivariable model calibration procedure (Seibert, 2000), where a combination of two criteria is defined as the objective function. These criteria are the model efficiency for SWE (NSE_{SWE} ; Nash & Sutcliffe, 1970) and the mean absolute normalized error for SWE (MNE_{SWE}), expressed as follows:

$$\text{NSE}_{\text{SWE}} = 1 - \frac{\sum (h_{\text{obs}} - h_{\text{sim}})^2}{\sum (h_{\text{obs}} - \bar{h}_{\text{obs}})^2} \quad (1)$$

$$\text{MNE}_{\text{SWE}} = 1 - \frac{\sum |h_{\text{obs}} - h_{\text{sim}}|}{\sum h_{\text{obs}}} \quad (2)$$

where h_{obs} and h_{sim} are the observed and the simulated snow water equivalent. The objective function is a combination of these two criteria giving the same weights to each of them. The aim was to reproduce the current snow accumulation and melt in order to get reliable future simulations. The model was validated using data from 2015 to 2018. Snow conditions did not change significantly during this period. Different calibration trials might result in different parameter sets with similar model performances during calibration but different behavior during other periods. To better address this parameter uncertainty, the model was calibrated 10 times starting each time from different initial parameter sets and resulting in 10 “best” parameter sets (for the search range of the snow parameters see Table S1 in the Supplementary Material). These 10 sets were then used to simulate 10 different time-series for all simulation periods. Most of the further analyses were then based on these 10 series for both reference and future periods.

Additionally, during snow parameter calibration a check was made to ensure no unrealistic snow accumulation series were modelled, as already observed with the HBV snow routine in the past (Jenicek et al., 2018). For this step, any simulation resulting in multi-year snow accumulation (snow tower building up, Freudiger et al., 2017) is assumed to be unrealistic. If it was the case, the initial search ranges for the snow parameters were arbitrarily reduced, within their range of variation, to avoid this artifact.

The NSE coefficient varies between $-\infty$ and 1, with a value of 1 representing a perfect reproduction of the time-series and a negative value indicating that the model performs worse than the simplest possible model, which is taking the average observed value as a model. It is important to point out here that this NSE value, if computed on strongly seasonal signals, needs to result in very high values to indicate good model performance (Schaeefli and Gupta, 2007). This explains the very high NSE_{SWE} values (> 0.90) obtained for all case studies (Table 3).

3.3.2.2. Soil and groundwater parameter calibration. In a second step, the model is calibrated to reproduce observed streamflow from the beginning of the monitoring period (see Table 1 for monitoring period per catchment) until 31 August 2015, as the last three years of measurements (2015–2018) are used for validation (see below). All parameters (except the snow ones) are calibrated using the inverse

Table 3

Mean values of the 10 objective functions obtained for the calibration of the snow water equivalent per catchment.

Catchment number	Snow parameter calibration		
	NSE_SWE	MNE_SWE	Period
#1	0.95	0.84	2015–18
#3	0.98	0.88	2015–18
#6	0.87	0.76	2015–18
#7	0.94	0.83	2015–18
#9	0.87	0.74	2015–18
#10	0.95	0.81	2015–18
#11	0.96	0.83	2015–18
#12	0.90	0.77	2015–18
#13	0.93	0.79	2015–18

automatic calibration software PEST (Doherty, 2005). PEST is a model-independent, non-linear parameter estimation and optimization package. It reads files of input parameters and target outputs. The algorithms are based on the implementation of the Gauss–Marquardt–Levenberg algorithm to allow a fast and efficient convergence towards the best value of the objective function. It is the minimum of a weighted least square sum of the difference between simulated and observed discharge. Calibration is conducted to reproduce streamflow with a specific interest in low flows using the following objective function ϕ :

$$\phi = \sum_{i=1}^n ((Q_i^{obs} - Q_i^{sim}) * w_i)^2 \quad (3)$$

where Q_i^{obs} and Q_i^{sim} are the observed and simulated catchment streamflow rates and w_i is the weight associated with the streamflow value at the time step i . Accordingly, higher weights are used on low flows (see supplementary material Table S3 for weights). PEST approaches an optimized parameter set within the specified ranges of the parameters (Doherty and Johnston, 2003). The optimization algorithm is run once for each of the ten best snow parameter sets identified in the previous set, resulting in a total of ten optimized parameter sets per catchment. Because it is a non-unique problem, different initial parameters are used to avoid the stay in the local minima of the objective function. These ten parameter sets were considered as representative of catchment variability in response to extreme climate change scenarios because the variability of parameters, and especially recession coefficients, are well constrained by the higher weight on winter low flows during a long period of time.

To assess the quality of the calibration, the mean flow rate volumetric error (MNE_Q), the Nash-Sutcliffe efficiency for discharge (NSE_Q) and for $\log(Q)$ (NSE_{lnQ}) between observed and simulated streamflow are calculated on the calibration period and on a three years validation period (2015–2018). They are expressed as follows:

$$NSE_Q = 1 - \frac{\sum_{i=1}^n (Q_i^{obs} - Q_i^{sim})^2}{\sum_{i=1}^n (Q_i^{obs} - \bar{Q}_{obs})^2} \quad (4)$$

$$NSE_{lnQ} = 1 - \frac{\sum_{i=1}^n (\ln Q_i^{obs} - \ln Q_i^{sim})^2}{\sum_{i=1}^n (\ln Q_i^{obs} - \bar{\ln Q}_{obs})^2} \quad (5)$$

$$MNE_Q = 1 - \frac{\sum_{i=1}^n (|Q_i^{obs} - Q_i^{sim}|)}{\sum_{i=1}^n (Q_i^{obs})} \quad (6)$$

where Q_i^{obs} and Q_i^{sim} are the observed and simulated catchment streamflow rates at the time step i . These three indicators (Eqs. (4), (5) and (6)) are not used as objective functions, but are rather calculated to evaluate the quality of the calibration performed with PEST. 1. The mean performance of the ten model runs with the optimized parameter sets are presented in Table 4 and Table 5 for the calibration and the validation period. The three coefficients indicate good overall model

Table 4

Value of the three streamflow performance measures calculated on the calibration periods per catchment.

Catchment number	Calibration			
	NSE_Q	MNE_Q	NSE_{lnQ}	Period
#1	0.72	0.84	0.69	2013–15
#3	0.67	0.80	0.81	1961–2015
#6	0.76	0.88	0.88	1990–2015
#7	0.70	0.81	0.84	1967–2015
#9	0.66	0.62	0.66	1977–2015
#10	0.55	0.62	0.71	1966–2015
#11	0.57	0.92	0.72	1961–2015
#12	0.67	0.97	0.78	1970–2015
#13	0.62	0.68	0.59	1963–2015

Table 5

Value of the three streamflow performance measures calculated for the validation periods per catchment.

Catchment number	Validation			
	NSE_Q	MNE_Q	NSE_{lnQ}	Period
#1	0.79	0.87	0.79	2015–18
#3	0.62	0.79	0.58	2015–18
#6	0.84	0.91	0.91	2015–18
#7	0.68	0.71	0.89	2015–18
#9	0.55	0.57	0.66	2015–18
#10	0.50	0.51	0.63	2015–18
#11	0.79	0.92	0.74	2015–18
#12	0.56	0.82	0.69	2015–18
#13	0.69	0.68	0.53	2015–18

performances for both periods, even with a higher weight on low flows in the objective function, as the model simulates satisfactory both high and low streamflow (i.e. values NSE_Q , NSE_{lnQ} and MNE_Q between 0.5 and 1).

3.4. Low-flow indicators

Low-flow indicators are used to compare the catchments regarding their potential to store groundwater. The $Q95/Q50$ (discharge exceeded 95% of the time divided by median discharge) ratio has already been used in low-flows studies in Swiss catchments (Carlier et al., 2018, 2019). These authors showed that large dynamic groundwater storage ensures high groundwater contribution during low flows and high $Q95/Q50$ ratios. In alpine catchments, as the winter low-flow period is long compared to the low-flow period of catchments with more rainfall-driven hydrological regimes (from 4 to 9 months for our studied catchments, depending on the snow cover duration), the winter flow index (WFI) is often used (Cochand et al., 2019b; Hayashi, 2020; Paznekas and Hayashi, 2015). These authors have shown that WFI can reflect the groundwater contribution to streamflow, a higher WFI indicating more groundwater contribution (Cochand et al., 2019b; Paznekas and Hayashi, 2015). It is here obtained as follows:

$$WFI = Q_{NM7}/Q_{mean} \quad (7)$$

where Q_{NM7} is the minimum discharge over seven consecutive days during the winter period (from November to June) and Q_{mean} is the mean annual discharge. We follow the definition from the paper of Cochand et al. (2019b). It is important to note that this study used a slightly different definition of the WFI: Paznekas and Hayashi (2015) used the specific average flow for January and February while Cochand et al. (2019b) used the minimum discharge over seven consecutive days. This latter definition is considered to be more appropriate given the variability of the studied catchments and to be able to compare them between each other. For many of the catchments, the low flow

period varies from February to June. Similarly to WFI, the summer low-flow index (SFI) is calculated with the Q_{NM7} in the summer months (from July to September).

Besides, as the main period of groundwater storage increase is during snowmelt, we decided to use also the obtained Dynamic Groundwater Storage (DGS) divided by the mean maximum snow water equivalent (DGS/SWE_{max}) as an indicator of groundwater contribution to streamflow for alpine catchments. This DGS is calculated from the model simulations and is the difference between the minimum and maximum groundwater level in the two combined groundwater reservoirs described above (upper and lower). These water levels computed by the model are not calibrated with, or compared to measured groundwater levels. There are no piezometers in most of the study catchments. Moreover, the groundwater boxes of the model do not represent a specific aquifer and cannot be compared to a point measurement such as water level in a piezometer. Two different DGS components are defined: DGS_n during the recharge period (from low to high level) and DGS_{n+1} during the recession period (from high to low level). They are expressed as follows:

$$DGS_n = H_n - h_n \quad (8)$$

$$DGS_{n+1} = H_n - h_{n+1} \quad (9)$$

where H_n is the maximum groundwater level in the combined upper and lower groundwater reservoirs (see Section 3.3.1.) of the year n , h_n is the minimum of the same year n , and h_{n+1} is the minimum of the following year. The mean DGS is the mean of both DGS_n and DGS_{n+1}.

DGS and SWE_{max} used in the index are both mean values calculated over the entire period of simulation based on historical data (calibration and validation periods). DGS/SWE_{max} varies between 0.3 and 0.8 for our catchments. A DGS/SWE_{max} close to 1 means that the majority of snowmelt contributes to groundwater storage. The low-flow indicators presented here are summarized in Table 6.

4. Results and discussion

In the following, we first compare the low-flow characteristics of all selected catchments with the surface geology. Then, we analyze the evolution of discharge in response to climate change scenarios. In this part, we focus on relative changes between the reference period and the future periods rather than absolute changes in simulated discharge to be able to compare the catchments between each other.

4.1. Relationship between low-flow behavior and geology

4.1.1. Low-flow indicators

The low-flow indicators, Q95/Q50, WFI and DGS/SWE_{max} are strongly positively correlated (Fig. 3 and detailed values in the Supplementary Material Table S4), i.e. if the DGS/SWE_{max} increases, the WFI (Fig. 3) and the Q95/Q50 (not shown) increase. This relationship confirms the previous findings (see Section 3.4) that catchments with high WFI, Q95/Q50 and DGS/SWE_{max} are those catchments that have a high groundwater contribution to streamflow, relative to the amount of precipitation they receive.

Given the strong correlation of the two low-flow indicators based on

historical data, Q95/Q50 and WFI (Fig. 3a), we only consider WFI in the rest of the study. The correlation between the data-based WFI and the model-based DGS/SWE_{max} is expected because an important flow rate after a prolonged winter recession requires a high dynamic groundwater storage in the model. This nevertheless gives confidence in the DGS/SWE_{max} indicator, which is based on a simple hydrological model, albeit calibrated with a special focus on low flows.

The range of variation of WFI is surprisingly high given that they are all alpine catchments with snow-dominated hydrological streamflow regimes but without significant glacier cover. It varies between 0.08 for #8 and #10 and 0.34 for #11 (Fig. 3). Based on these values, three clusters of similar values can be defined: catchments #11, #1, #12 and #2 have a high groundwater storage potential ($0.25 \leq WFI < 0.35$), catchments #3, #4, #13, #5, #6 a medium ($0.15 \leq WFI < 0.25$) and catchments #7, #10, #9 and #8 a low ($0 \leq WFI < 0.15$). In the literature, WFI varies between 0.05 and 0.28 for large alpine catchments (drainage areas $> 250 \text{ km}^2$; Hayashi, 2020) and between 0.28 and 0.10 for some Swiss alpine catchments (Cochand et al., 2019b).

4.1.2. Low-flow indicators and geology

Both WFI and DGS/SWE_{max} are positively correlated with the relative amount of Quaternary deposits (Fig. 4). Hence the results highlight the importance of unconsolidated Quaternary deposits, such as moraines, alluvium, and talus, in storing groundwater. These deposits are typical for alpine areas. This result gives evidence for the fact that in the Swiss Alps, the seasonal groundwater storage is strongly influenced by the local geology, even if more catchments would be required to statistically validate this relationship. Other groundwater systems, such as karstic or fractured bedrock systems, can also jointly interact with Quaternary deposits to store groundwater. For example, for catchment #1, an evaporitic zone and Quaternary deposits contribute significantly to winter low flows (Cochand et al., 2019b). For catchment #12, weathered bedrock and Quaternary deposits contribute significantly to winter low flows (Floriancic et al., 2018), this could explain why it plots toward higher WFI in Fig. 4a.

The recent literature review of Hayashi (2020) highlights the important role of Quaternary deposits in storing groundwater in alpine regions. It has been shown that groundwater storage can be controlled by the combination of Quaternary deposits, for example, talus and meadow in the Andean mountains (Glas et al., 2019) or talus and moraine in the Swiss Alps (Cochand et al., 2019b). In a recent review, Hayashi (2020) hypothesized that groundwater storage in alpine areas is probably controlled by the combination of bedrock topography covered by Quaternary deposits or by the permeability variation inside moraines and talus. We suggest that another reason explaining the importance of unconsolidated deposits is that they prevent fast runoff of melt and rainwater, thus maintaining groundwater recharge irrespectively of the aquifer type that is responsible for groundwater storage. This mechanism could be particularly important for recharge of fractured bedrocks, which often feature limited infiltration capacity thus normally favoring runoff. However, it is important to note that the surface slopes could indirectly affect subsurface and surface hydraulic gradients and hence the rates at which the water is drained out of the system. The mean slope and the percentage of Quaternary deposits are both intrinsically linked: the mean slope increases when the percentage

Table 6
Summary of the low-flow indicators.

Low-flow indicator	Definition	Data used to calculate it in the paper
Q95/Q50	Mean discharge exceeded 95% of the time divided by mean median discharge	Measured discharge
WFI	Mean winter minimum discharge over seven consecutive days divided by the mean annual discharge	Measured discharge
DGS/SWE _{max}	Mean dynamic groundwater storage divided by the mean maximum snow water equivalent	Data obtained from the simulation of historic discharge
SFI	Mean summer minimum discharge over seven consecutive days divided by the mean annual discharge	Future simulated discharge

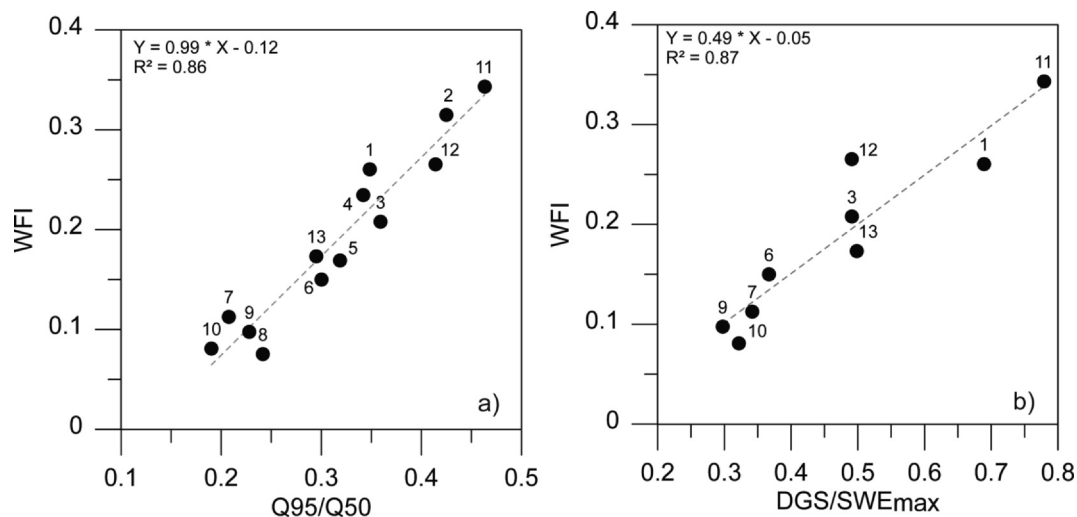


Fig. 3. The three low-flow indicators for the study alpine catchments; (a) WFI and Q95/Q50 are calculated from measured discharge (13 catchments) and (b) DGS/SWEmax is obtained from the model (9 catchments).

of Quaternary deposits decreases and the role of slope cannot be distinctly explored (see Fig. S4 in Supplementary Material).

Following the discussion concerning the role of unconsolidated Quaternary deposits in storing groundwater, their hydrologic response to climate change is further explored and associate with geological conditions and storage dynamics.

4.1.3. Streamflow with past meteorological conditions (1968–2017)

Meteorological changes from 1968 to 2018 are as follows (data not shown): mean annual precipitation stays constant, the temperature increases, evaporation increases but stays small (mean ET from 170 to 300 mm/yr depending on the catchments).

Observed historical streamflow data and corresponding SWE data are presented for some of the catchments to determine whether relevant changes in seasonal streamflow can already be observed in response to the increase in air temperature during recent decades (Fig. 5). The changes in observed discharge are compared with changes in simulated SWE on two 30-year mean periods, for the catchments with a long period of streamflow monitoring (Fig. 5).

The results of the simulations show a decrease in mean simulated SWE for all catchments (Fig. 5 b). Maximum SWE on a 30-year average

follows a decrease for all catchments, ranging from approx. –65 mm to –140 mm in May (#11) or June (#7, #3) over the 1988–2017 period compared to the 1968–1999 period (Fig. 5 b). As shown in Fig. 5a, the streamflow increases in May and decreases in July because snowmelt starts and finishes earlier in the year. Thereafter, streamflow decreases in the summer months from July to September or to October and increases for the rest of the year. Overall, the mean annual streamflow remains constant throughout the years (except a slightly positive annual trend for catchment #7).

4.2. Discharge evolution with climate change

In the following, the annual and seasonal evolutions of discharge under climate change scenarios and the factors influencing it are described and discussed. The aim is to link the discharge regime evolution in response to climate change and groundwater storage, and therefore, geology.

4.2.1. Mean annual changes

As expected, all catchments are affected by a decrease in snow water equivalent in the future periods for the three scenarios due to the

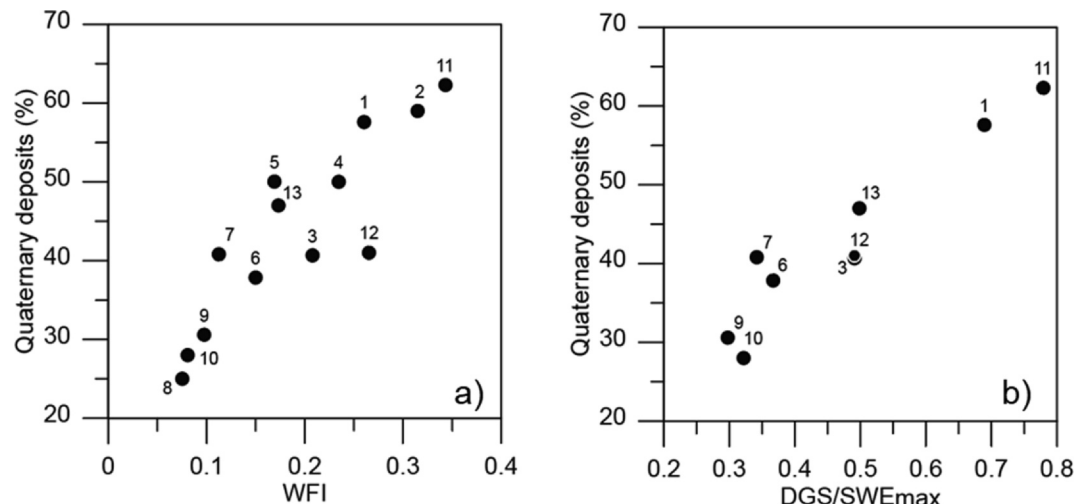


Fig. 4. Percentage of Quaternary deposits versus low-flow indicators WFI (a) and DGS/SWEmax (b); WFI is calculated from measured discharge (13 catchments) and DGS/SWEmax is obtained from the model (9 catchments). The percentage of Quaternary deposits is determined based on the GeoCover dataset (1: 25'000) from SwissTopo.

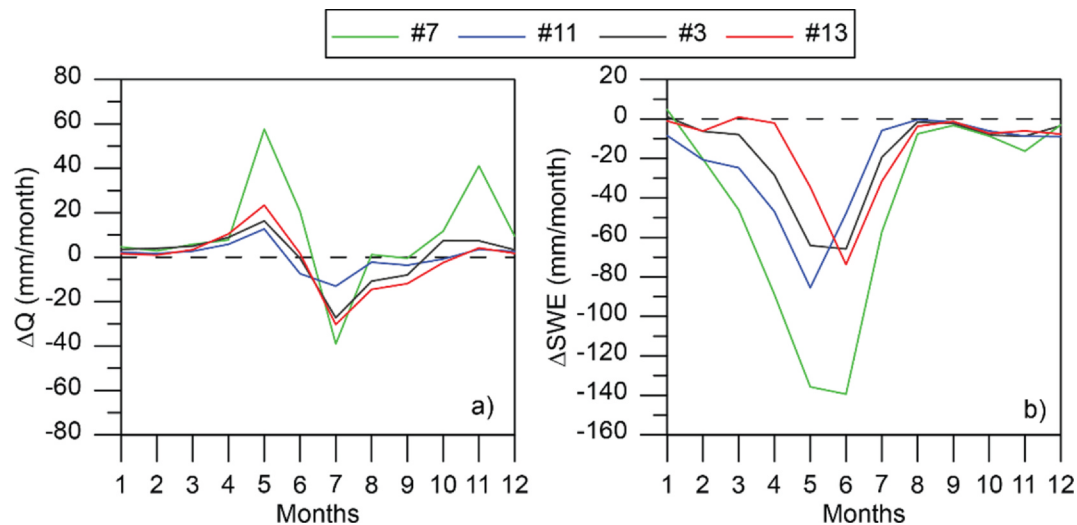


Fig. 5. Change of (a) the monthly mean measured streamflow (Q) and (b) simulated monthly mean snow water equivalent (SWE) of the 30 years 1988–2017 compared to the 30-year reference 1968–1999 (years 1977 and 1978 are not considered because of a lack of data for one catchment), for four of the study alpine catchments.

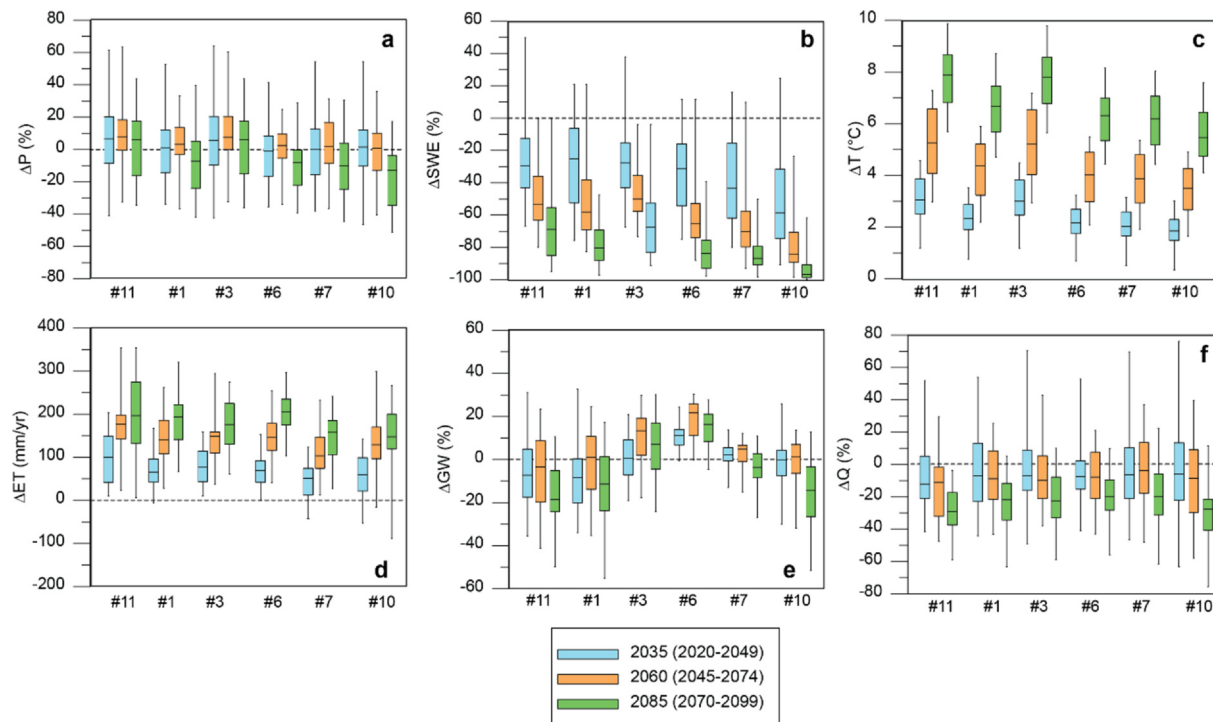


Fig. 6. Change in mean annual precipitation (a), snow water equivalent (b), temperature (c), evapotranspiration (d), groundwater storage (e), streamflow (f) for catchments #11, #1, #3, #6, #7 and #10 for the 3 future periods: 2035 (2020–2049) in blue, 2060 (2045–2074) in orange and 2085 (2070–2099) in green, compared to the reference period (1982–2011) for only scenario S3. Scenarios S1 and S2 are shown in Supp Mat. S1.

increase of air temperature during spring and winter. Both the reduction of snow cover duration and the rise in the air temperature increase the potential evapotranspiration. The simulated actual evapotranspiration increases from 150 mm/year for the reference period (from 1982 to 2011) to 200 mm/year by the 2085 period for the studied catchments (data not shown). Future evapotranspiration represents, for some catchments, twice the actual evapotranspiration in the reference period (ex. catchment #6 from 200 to 400 mm/yr by the end of the century with S3, Fig. 6 d). However, the calculated evapotranspiration is limited regarding the increase in air temperatures because of shallow soils in alpine areas. Not taking into account the depth of soils in alpine areas, the annual evapotranspiration remains limited but can still

become an important factor in the annual water budget in alpine areas in the future.

In Fig. 6, the results of the parameters for the simulation of six catchments for S3 are shown. The catchment selection is based on their WFI values. The selected catchments have WFI values covering the full range of variation, from 0.08 (#10) to 0.34 (#11), with #1, #3, #6 and #7 between.

The response of the mean annual streamflow to climate change varies for different scenarios and catchments. All catchments show a decreasing trend in mean annual streamflow by the 2085 period. This decrease ranges from approx. -150 mm/yr for catchments #11 and #3 to -400 mm/yr for catchments #6 and #10. It represents a streamflow

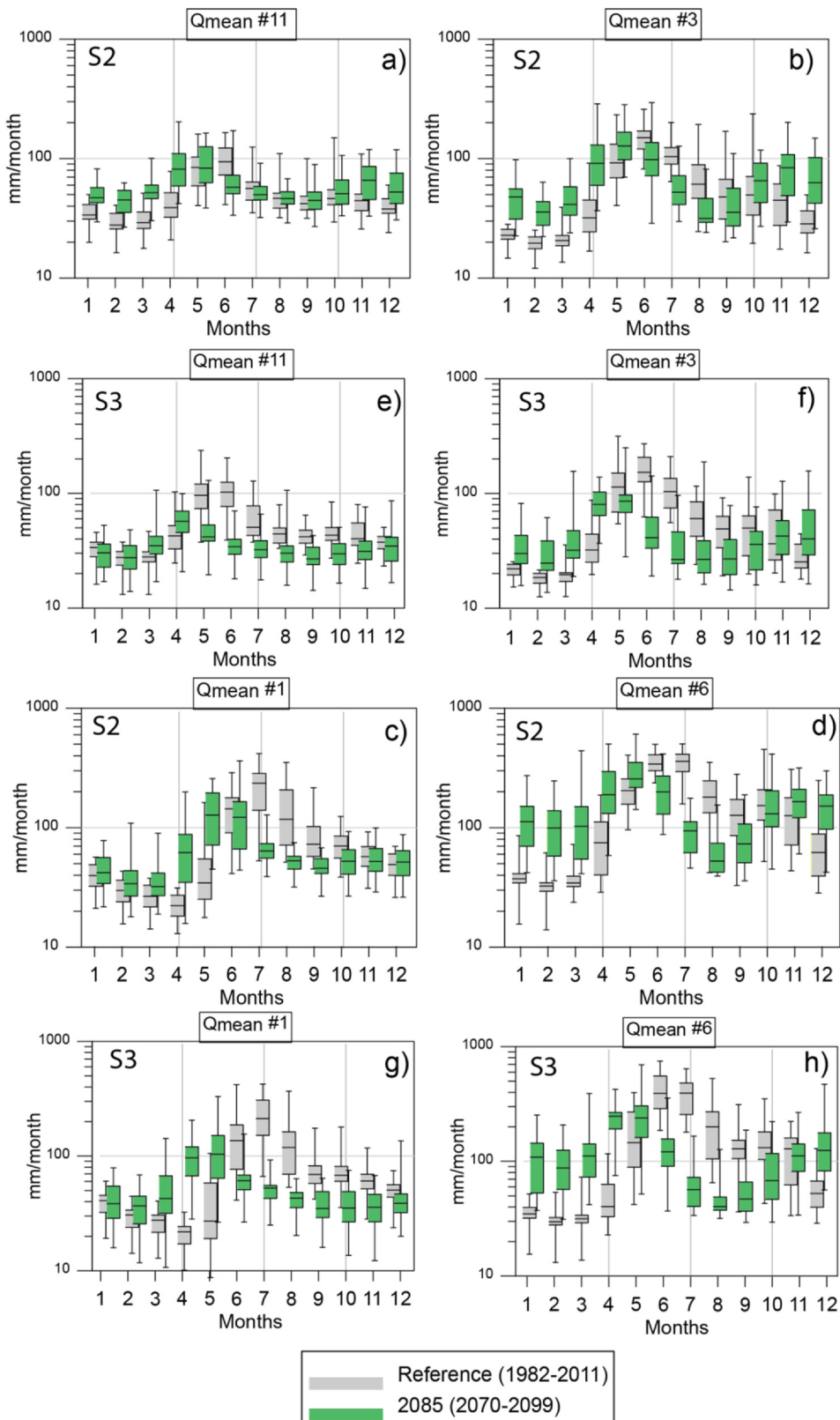


Fig. 7. The seasonal variation of monthly mean streamflow (Q_{mean}) for the future period 2085 and the reference period. The four catchments presented here cover a broad range of WFI values, from high to low: #11, #1, #3 and #6. Two RCP8.5 scenario simulations are presented S2 and S3.

decrease by -20% for #6 and -30% for #10 and #11). These changes can be mainly explained by a decrease in precipitation (Fig. 6 a) affecting all catchments for the 2085 period (maximum decrease of 16.5% in mean for #10), except catchments #3 and #11, which show

an increase in annual precipitation ($+1.4$ and 0.9% in mean, for #3 and #11, respectively). A further explanation for streamflow reduction is the continuous increase in evapotranspiration, as it is the case for #11 and #3.

Groundwater storage shows similar variations as streamflow, with a slight decrease for the 2085 period (from -10 to -20% in mean), except for catchments #3 and #6 for which mean groundwater storage increases by + 10 to 15% for the 2085 period, respectively (Fig. 6 e). To explain these annual variations, it is necessary to analyze the seasonal variations of groundwater storage and streamflow.

With scenarios S1 and S2, mean annual streamflow and groundwater storage do not show significant trends or follow a slight increase for the 2085 period, compared to the reference period (data not shown).

4.2.2. Mean seasonal variations

The seasonal variations are compared between the reference and the 2085 period. Future precipitation patterns between the three scenarios S1-S3 are as follows: for S1, mean seasonal precipitation stays relatively constant (except for catchments #3 and #11 where they slightly increase in summer); for S2, precipitation increases in winter and slightly decreases in summer (except for catchments #3 and #11 where precipitation stays constant in summer); and for S3, precipitation stays relatively constant during winter and decreases in summer (detailed plots available in Supplementary Material, Fig. S2).

The simulated evapotranspiration increases mainly during spring due to earlier snowmelt and higher temperatures combined with high water availability in the soil (see Fig. S2). Future simulated evapotranspiration (ranging from few mm/month to 120 mm/month in the 2085 period) can significantly reduce water availability for streamflow in summer.

The simulated SWE_{max} is lower and appears 1 to 2 months earlier for all catchments and scenarios (Fig. S2). In response, streamflow peaks and the main recharge period occur 1 to 2 months earlier and the maximum streamflow decreases.

The simulated groundwater storage increases in winter because of a shorter mean snow cover period and therefore a longer period for recharge. For scenario S3, the mean groundwater storage decreases in summer for the 2085 period for most of the catchments. For scenarios S1 and S2, the summer groundwater storage increases (for catchments #6, #9, #11, #3, #13) or decreases (catchments #1, #7, #12 and #10; Fig. S2). This increase is due to the melt recharge during winter and spring and partly due to an increase in summer precipitation (for example, for catchments #3 and #11 with S1). The groundwater minimum tends to shift from winter to summer for the 2085 period.

The differences in scenarios S3, S2, S1 highlight the fact that groundwater storage also depends on spatial precipitation patterns. To summarize, for all scenarios and catchments, for the 2085 period relative to the reference period, the differences in groundwater storage are the following: (1) a lower decrease in winter, (2) a lower and earlier recharge during the melt period, (3) a more pronounced decrease in summer, and (4) a higher increase in autumn due to more liquid precipitation.

Based on the simulations, the fraction of streamflow originating from snowmelt to total streamflow in June and July decreases for the 2085 period and almost completely disappears at the lowest elevations (for example, catchment #10). As mentioned earlier, the climate change scenarios selected for this study represent a strong warming trend and therefore entail a strong reduction in snowmelt. However, the evolution of snowmelt and corresponding streamflow generation is still in agreement with what has already been shown in previous studies (e.g. Jenicek et al. 2018). Consequently, the impact of snowmelt on streamflow in alpine catchments will not be discussed in detail in this paper. The decrease in summer streamflow is mainly influenced by the shift of the timing of snowmelt. For example, a decrease of 90% of streamflow in July and 80% in August is observed for #6 with S3 (Fig. 7h). The future summer streamflow depends on previous hydrological conditions, precipitation patterns, evapotranspiration, and groundwater contribution. For all scenarios and for all catchments, streamflow increases in winter (December to February), ranging from a

few mm/month to around 100 mm/month in January-February. Subsequently, for almost all catchments, streamflow decreases in summer from a few mm/month to around 50 mm/month in August-September (Fig. S2). Furthermore, snowmelt, precipitation, and groundwater maintain summer low flows higher than historic winter low flows. Current winter low flows, therefore, appear to form a lower bound for future summer low flows, as the mean future summer low flows stay above the current mean winter low flows. Moreover, the low-flow period starts to shift from winter to summer.

In Fig. 7, the discharges of four catchments are presented. The selection is based on their WFI range (from 0.15 to 0.34) and is also based on the availability of a gauging station above 1300 m a.s.l.. Furthermore, these catchments are interesting because they will continue to show a snowmelt-dominated regime even with the considered climate change scenarios. The other catchments are presented in the Supplementary Material (Fig. S2).

The differences in catchment responses in summer low flows due to their hydrogeological characteristics become more apparent for S3 than for S2 (Fig. 7) or for S1 (Fig. S2a). Indeed, in this scenario, the high flows are smaller and the recession durations are longer (Fig. 7). This is due to an earlier snowmelt peak because of higher temperatures in spring and no increase in summer precipitations (Table 2 and Fig. S2c).

In Fig. 8, the seasonal difference between reference and the 2085 period (ΔQ , ΔSWE and $\Delta[P-ET]$) of catchments #11 and #3 for scenarios S1, S2 and S3 are presented. These two catchments are discussed in more detail because they are both located close to each other in the east part of Switzerland at similar altitudes, with similar changes in P, T, and ET. For streamflow, the variations of #3 are higher than for #11 whereas variations of SWE (Fig. 8b and e) and [P-ET] (Fig. 8c and f) are similar for these two catchments.

In future scenarios, the changes in simulated streamflow in August can be described as follows:

- for S1, a decrease of 10% (7 mm/month) for #3 (Fig. 8a) and an increase of 11% (5 mm/month) for #11 (Fig. 8b);
- for S2, a decrease of 43% (30 mm/month) for #3 (Fig. 8a and Fig. 7b) and almost no change for #11 (Fig. 8b and Fig. 7a);
- for S3, a decrease of 45% (29 mm/month) for #3 (Fig. 8a and Fig. 7f) and of 29% (13 mm/month) for #11 (Fig. 8b and Fig. 7e).

These differences between #3 and #11 behaviors can be explained by the differences in groundwater storage and thus in geology. Facing a similar climatic evolution, catchment #11 has a slower decrease in discharge because of the buffer effect of groundwater. It is therefore able to maintain a similar quantity of water for a longer time without water input from rain or snowmelt. It is therefore less sensitive to climate change, as its changes in high or low flows are smoother than a catchment with lower groundwater storage potential, as catchment #3, in similar climate change conditions. However, it is important to note that we refer to relative changes and not to the absolute quantity of water available in the river which can also be relevant for water management. Besides, if a catchment is located in an area with an increase in precipitation during summer, these differences cannot be identified.

4.2.3. Predictions of future summer low flows and geology

Given the importance of future low-water periods in alpine areas, we provide some useful elements to better predict their future dynamics. We have shown that, even in the far future, summer low flows are not as extreme as current winter low flows in alpine catchments because their duration is shorter (between 2 and 4 months) and recharge by precipitation occurs. In the studied catchments, streamflow is provided for 4 to 9 months without precipitation input, as shown by historically measured streamflows. Therefore, the current winter low flow constitutes a lower bound for the future summer low flow.

The comparisons between WFI (based on historical data) and future

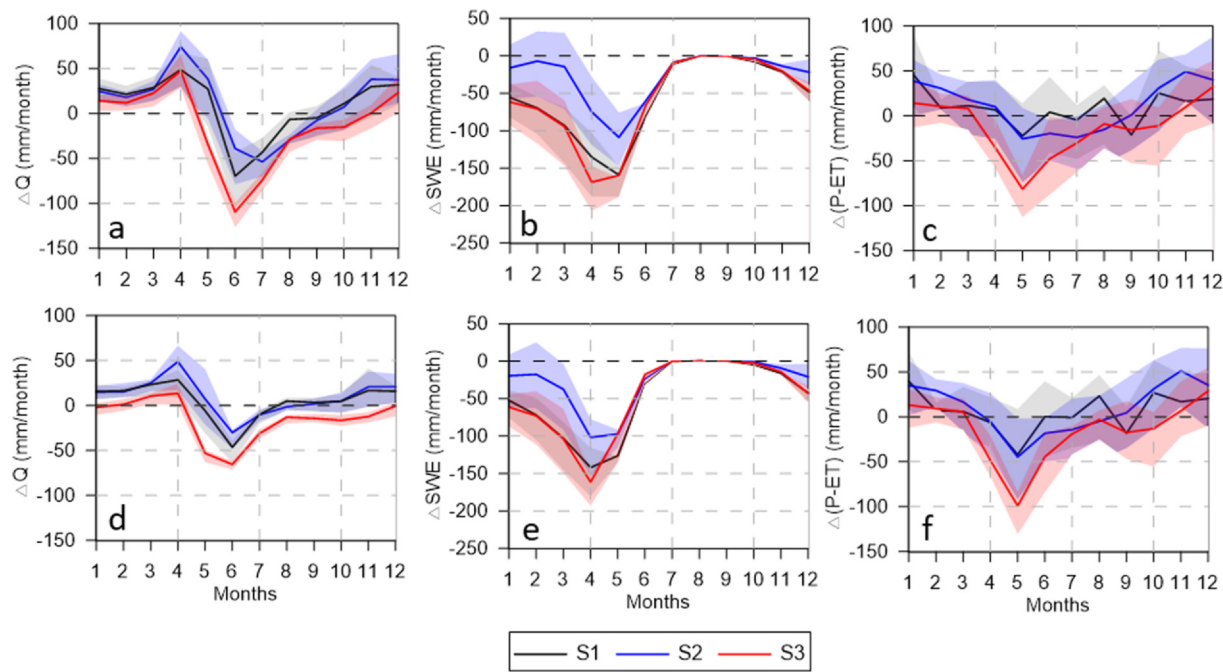


Fig. 8. The monthly relative changes of streamflow (Q; a and b), SWE (b and e) and precipitations-evapotranspiration (P-ET; c and f) for catchments #3 (top) and #11 (bottom) in the 2085 period (2070–2099) regarding the reference period (1982–2011). The three RCP8.5 scenarios simulations are presented here, S1 (black), S2 (blue) and S3 (red); the envelopes represent the first and third quartiles in 2085 compared to the mean reference.

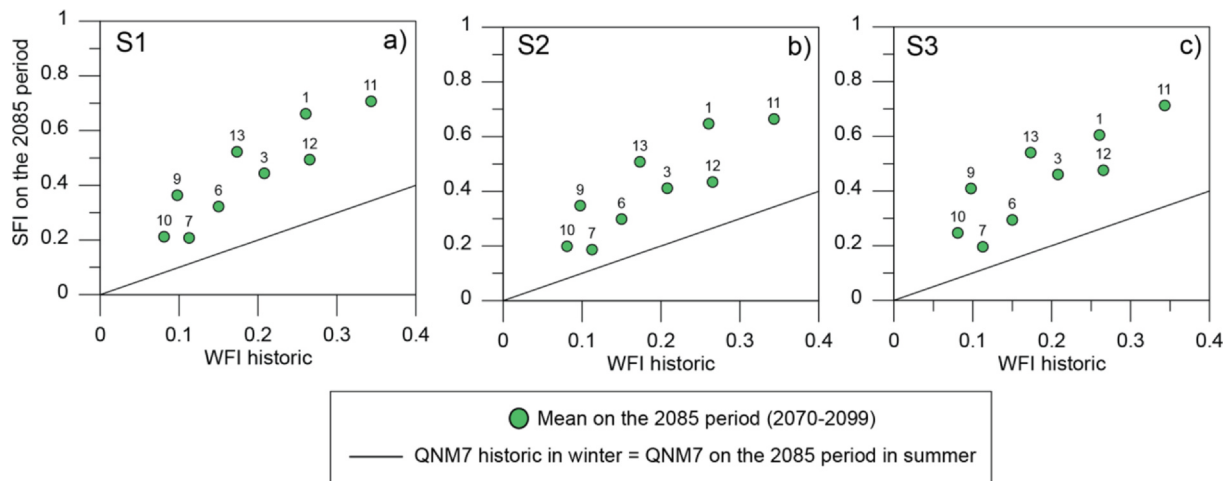


Fig. 9. SFI for the 2085 period for a) S1, b) S2, and c) S3, versus WFI historic calculated on the catchments' monitoring periods.

2085 SFI (mean on 30 years on the 2085 period) for the three scenarios are presented in Fig. 9 (the future Q_{NM7} and Q_{mean} used to obtain SFI are presented in the Supplementary Material, Fig. S3). The current winter low flow appears as a reliable indicator of future summer low flows: a catchment with a higher WFI will also have a higher SFI in the future. The future SFI stays higher than historic WFI for all catchments but trends are similar between both indicators. It means that SFI varies also with the percentage of Quaternary deposits of the catchments. Therefore, catchments with a higher percentage of Quaternary deposits will probably have a slower decrease in summer low flows, relative to the precipitations they receive. Therefore, the percentage of Quaternary deposits could be another indicator in addition to the current winter low flows, for future summer discharge projections.

In terms of quantity, future groundwater exfiltration accounts for significantly less water (a few cm/month) than current snowmelt (more than a hundred mm in a month) and thus cannot mitigate the effect of change in snowmelt due to climate change during the current period of

snowmelt. Therefore, a strong decrease in summer flows will most probably be observed at the beginning of summer (June-July). Thus, during future summer low flows, the SFI remains higher than WFI for all catchments (Fig. 9). For example, a $SFI > 0.5$ (#1 and #11) means that even under future conditions, the low flow is at least half the average flow. The SFI is fairly similar between the three scenarios because it represents the hydrogeological characteristics of the catchments. However, even with a high SFI, the decrease in future summer low flows can be significant for water management, in terms of absolute quantity.

We have seen in the previous analysis of seasonal variations of streamflow under climate change, that conditions similar to the scenario S3 favour a stronger influence of hydrogeological catchment characteristics on summer low flows (Fig. 7 and Fig. 8). These conditions are a strong increase in temperature and a decrease in summer precipitation without much increase in winter precipitation. In such a climate change scenario and for similar climatic conditions, the

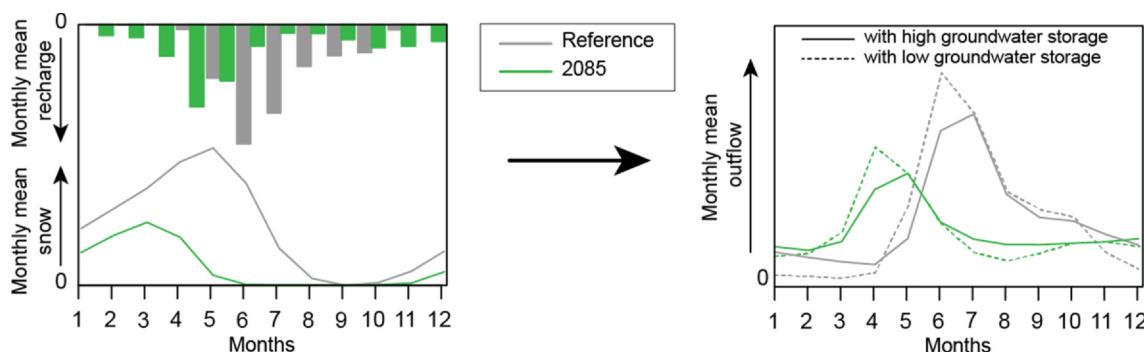


Fig. 10. Conceptual schema of stream discharge evolution in the future with a strong increase of temperatures and decrease in summer precipitations highlighting the buffer role of groundwater.

streamflow of an alpine catchment with a higher percentage of unconsolidated Quaternary deposits, and therefore higher storage, will follow a lower decrease in future summer, as illustrated in Fig. 10.

5. Limitations

Groundwater dynamics are highly simplified in the conceptual hydrological model employed here, which considers two linear groundwater reservoirs, one fast and one slow. In high elevation catchments, the approach can be justified because, during the winter low-flow period, i.e. the snow-covered period, only groundwater is contributing to streamflow. In this case, the groundwater reservoirs can be considered as linear and recession coefficients can be more easily calibrated (Santos et al., 2017). However, in reality, alpine aquifers behave in a non-linear way, owing to their heterogeneity and complex geometry. Moreover, our analysis of geology could be improved by information on the thickness and the hydrogeological characteristics of the different deposits such as alluvium, talus or moraine which would also play a role in the storage and the release of groundwater. More information about the geology of the catchment is needed to improve this work and to validate the assumption that there is no groundwater flowing under gaging stations. This work could be improved with a 3D geological model, however, the establishment of such a detailed model is very time consuming and often cannot be built with the available information (Thornton et al., 2018). Furthermore, Quaternary deposits have smaller slopes than crystalline rocks and slopes could indirectly affect hydraulic gradients. Therefore, there may be some interplay between slope and the rate of groundwater drainage out of the catchment and it would need more investigation.

Moreover, some aquifers with lower permeability than unconsolidated Quaternary deposits, such as bedrock, can control long-term discharge dynamics (Carlier et al., 2018) and therefore the responses to climate changes. The long-term responses to changes are not taken into account in such conceptual models. In some geological settings (e.g., extrusive volcanic rocks; e.g., Andes and Cascades Ranges) the permeability of the hard rock parts of the alpine system can be much higher than that of the mostly fractured crystalline rocks examined in this study. In turn, the role of geology in buffering or modifying system response to climate change may be even more profound and requires more investigation. Therefore, hydrogeological modeling in alpine areas should be developed in a physically-based manner to better determine the role of groundwater in buffering streamflow regime changes.

We also assumed that the model calibration is transferable to future climate scenarios, which may not entirely be the case, in particular into the far future with extreme scenarios. Moreover, only changes in precipitation and temperature are considered; the evolution of other parameters, such as vegetation cover, frozen soils or increase in water needs, are not considered. It is also important to note that the studied catchments do not contain glaciers (or only a small remnant),

consequently, the results may not be comparable to other studies that involve runoff from glacierized catchments.

6. Conclusions

The interplay of snow storage and catchment-scale groundwater storage significantly influences how alpine catchments react to ongoing climate warming. The main objectives of this study were (1) to investigate the similarities and the differences in low-flow behaviour between Alpine catchments and to compare the relationship of low-flow regimes with catchment geology, (2) to determine if groundwater storage can buffer future summer low flows, and (3) to establish a link between geology and catchments responses to climate change. The analysis was based on 13 selected catchments across the Swiss Alps with reliable streamflow measurements. The analysis was completed in two steps by first comparing well established low-flow indicators to surface geology and then simulating past and future streamflow with a simple conceptual hydrological model, in which three of the latest extreme RCP8.5 CH2018 climate change scenarios were used.

The results of the data analysis clearly indicate a relationship between geology and the low-flow indicators for the studied Swiss catchments: catchments with more Quaternary deposits are able to provide more water during low-flow periods. However, a larger set of study catchments would be required to statistically validate this relationship between low-flow indicators and geology. Nevertheless, these results agree with the recent literature showing the important role of Quaternary deposits in storing groundwater in alpine catchments. Three mechanisms could explain this importance of Quaternary deposits: i) the combination of Quaternary deposits with various permeabilities can store enough water to release it slowly during drier years (Cochand et al., 2019b; Glas et al., 2019; Hayashi, 2020); ii) Quaternary deposits filling bedrock depressions which act as barriers to flow allows the storage of significant amount of groundwater; and iii) the high permeability of these water-storing deposits facilitate deeper infiltration to layers with lower permeability such as fractured bedrock. In fact, such deep infiltration is probably less efficient without Quaternary deposits, especially on steep slopes. The dominant role of Quaternary aquifers underlines that first-order watersheds are elementary units for characterizing alpine hydrogeology. Their correct conceptualization in numerical models is essential.

Based on these findings, we calibrated the hydrological model with a special focus on reproducing low flows. The results of our future simulations show the now well-known increase of streamflow during winter and decrease of streamflow during summer. We clearly show that the annual low-flow period starts to shift from winter to summer, as simulated future summer low flow is sometimes lower than future winter low flows. The impact of snowmelt on summer low flows decreases. These changing dynamics are explained by less snow and shorter snow cover periods. The results show that in response to the three considered climate change scenarios, the mean summer low flows

stay at least as high as the current mean winter discharge volume rate. The results also highlight that catchments with higher current groundwater contribution to streamflow will have a slower decrease in future summer discharge, relative to the precipitation they receive.

The simulation results also show that the future summer low-flow index is correlated to the current winter low-flow index, which we have shown to be correlated with the percentage of unconsolidated Quaternary deposits in the study alpine catchments. Therefore, we propose two indicators which can help to anticipate future summer low flows in alpine areas under climate change as a function of current winter low flows and of the percentage of Quaternary deposits. Future research should, however, deploy spatially distributed hydrogeological modeling to explicitly consider geology in assessing the role of groundwater for streamflow regime changes in an improved and quantitative way. The modelling of both, the 3D groundwater dynamic and surface hydrology, would be fruitful to improve our conceptual model of hydrogeological processes in alpine catchments. Such a 3D model requires, however, a good knowledge about the geology and its hydrodynamic properties, which have to be further explored. Building a 3D geological model is very time consuming (Thornton et al., 2018), therefore, a physical hydrogeological with a simplified geology to determine the role of quaternary deposits versus fractured bedrock and slopes could be a next step to improve knowledge in alpine hydrogeological processes and their evolution with climate change.

This study gives important insights into the evolution of groundwater storage and streamflow under future climate. Changes in streamflows need to be considered in water management adaptation strategies, since shifts to lower flows in summer combined with increased water needs could lead to water shortage. The decrease in water volume during summer will reduce water availability during the warm periods for uses such as hydropower, irrigation, and recreation. The increase of streamflow during winter could also be impactful for areas with increased winter water needs for ski tourism. Finally, this study also shows the importance of low flows and therefore the need for good low-flow measurements and model calibration for climate change projections, which is still not always the case within climate change impact studies in Alpine environments. As such, the role of groundwater and geology should be considered in future climate change impact projections.

CRediT authorship contribution statement

Marie Arnoux: Investigation, Methodology, Formal analysis, Writing - original draft, Writing - review & editing. **Philip Brunner:** Conceptualization, Supervision, Writing - review & editing, Project administration, Funding acquisition. **Bettina Schaeefli:** Conceptualization, Writing - review & editing. **Rebecca Mott:** Writing - review & editing. **Fabien Cochand:** Writing - review & editing. **Daniel Hunkeler:** Conceptualization, Supervision, Writing - review & editing, Project administration, Funding acquisition.

Declaration of Competing Interest

The authors declare that they have no known competing financial interests or personal relationships that could have appeared to influence the work reported in this paper.

Acknowledgments

We would like to acknowledge the Federal Office for the Environment of Switzerland (FOEN) and the Canton of Ticino for providing us reliable streamflow data, Meteoswiss for the RhinesD and TabsD products and the climate change CH2018 projections and SwissTopo for the geological maps. This work was funded by the FOEN, within the framework of climate change impacts on water resources in

Switzerland (HydroCH2018). The work of Bettina Schaeefli was supported by a research grant of the Swiss National Science Foundation (SNF, PP00P2_157611). We thank the Editor and two anonymous reviewers for their helpful feedback.

Appendix A. Supplementary data

Supplementary data to this article can be found online at <https://doi.org/10.1016/j.jhydrol.2020.125591>.

References

- Addor, N., et al., 2014. Robust changes and sources of uncertainty in the projected hydrological regimes of Swiss catchments. *Water Resour. Res.* 50 (10), 7541–7562. <https://doi.org/10.1002/2014wr015549>.
- Arnoux, M., Halloran, L.J.S., Berdat, E., Hunkeler, D., Characterising seasonal groundwater storage in alpine catchments using time-lapse gravimetry, water stable isotopes and water balance methods. *Hydrological Processes*, n/a(n/a). DOI:10.1002/hyp.13884.
- Barnett, T.P., Adam, J.C., Lettenmaier, D.P., 2005. Potential impacts of a warming climate on water availability in snow-dominated regions. *Nature* 438 (7066), 303–309. <https://doi.org/10.1038/nature04141>.
- Barnhart, T.B., et al., 2016. Snowmelt rate dictates streamflow. *Geophys. Res. Lett.* 43 (15), 8006–8016. <https://doi.org/10.1002/2016gl069690>.
- Beaulieu, M., Schreier, H., Jost, G., 2012. A shifting hydrological regime: a field investigation of snowmelt runoff processes and their connection to summer base flow, Sunshine Coast, British Columbia. *Hydrol. Process.* 26 (17), 2672–2682. <https://doi.org/10.1002/hyp.9404>.
- Beniston, M., Stoffel, M., 2014. Assessing the impacts of climatic change on mountain water resources. *Sci Total Environ* 493, 1129–1137. <https://doi.org/10.1016/j.scitotenv.2013.11.122>.
- Berghuijs, W.R., Woods, R.A., Hrachowitz, M., 2014. A precipitation shift from snow towards rain leads to a decrease in streamflow. *Nat. Clim. Change* 4 (7), 583–586. <https://doi.org/10.1038/nclimate2246>.
- Bergström, S., 1995. The HBV model (Chapter 13), in: Computer Models of Watershed Hydrology, edited by: Singh, V. P., Water Resources Publications, Highlands Ranch, Colorado, USA, 443–476.
- Bergström, S., 1976. Development and application of a conceptual runoff model for Scandinavian catchments, Bulletin Series A, No. 52, Department of Water Resources Engineering, Lund Institute of Technology, University of Lund, 134 pp.
- Carlier, C., Wirth, S.B., Cochand, F., Hunkeler, D., Brunner, P., 2018. Geology controls streamflow dynamics. *J. Hydrol.* 566, 756–769. <https://doi.org/10.1016/j.jhydrol.2018.08.069>.
- Carlier, C., Wirth, S.B., Cochand, F., Hunkeler, D., Brunner, P., 2019. Exploring geological and topographical controls on low flows with hydrogeological models. *Ground Water* 57 (1), 48–62. <https://doi.org/10.1111/gwat.12845>.
- Christensen, C.W., Hayashi, M., Bentley, L.R., 2020. Hydrogeological characterization of an alpine aquifer system in the Canadian Rocky Mountains. *Hydrogeol. J.* 28 (5), 1871–1890. <https://doi.org/10.1007/s10040-020-02153-7>.
- CH2018, 2018a. Climate Scenarios for Switzerland, Technical Report, National Centre for Climate Services, Zurich, 271 pp. ISBN: 978-3-9525031-4-0.
- CH2018, 2018b. CH2018 Project Team - Climate Scenarios for Switzerland. National Centre for Climate Services. doi: 10.18751/Climate/Scenarios/CH2018/1.0.
- Clow, D.W., et al., 2003. Ground water occurrence and contributions to streamflow in an alpine catchment, Colorado Front Range. *Groundwater* 41 (7), 937–950. <https://doi.org/10.1111/j.1745-6584.2003.tb02436.x>.
- Cochand, F., Therrien, R., Lemieux, J.-M., 2019a. Integrated hydrological modeling of climate change impacts in a snow-influenced catchment. *Groundwater* 57 (1), 3–20. <https://doi.org/10.1111/gwat.12848>.
- Cochand, M., Christe, P., Ornstein, P., Hunkeler, D., 2019b. Groundwater storage in high alpine catchments and its contribution to streamflow. *Water Resour. Res.* 55 (4), 2613–2630. <https://doi.org/10.1029/2018wr022989>.
- Cras, A., Marc, V., Travi, Y., 2007. Hydrological behaviour of sub-Mediterranean Alpine headwater streams in a badlands environment. *J. Hydrol.* 339 (3–4), 130–144. <https://doi.org/10.1016/j.jhydrol.2007.03.004>.
- Doherty, J., 2005. PEST Model-Independent Parameter Estimation User Manual. Watermark Numerical Computing, fifth ed. < <http://www.pesthomepage.org> > .
- Doherty, J., Johnston, J.M., 2003. Methodologies for calibration and predictive analysis of a watershed model. *J. Am. Water Resour. Assoc.* 39, 251–265. <https://doi.org/10.1111/j.1752-1688.2003.tb04381.x>.
- Florianic, M.G., et al., 2018. Spatio-temporal variability in contributions to low flows in the high Alpine Poschiavino catchment. *Hydrol. Process.* 32 (26), 3938–3953. <https://doi.org/10.1002/hyp.13302>.
- Freudiger, D., Kohn, I., Seibert, J., Stahl, K., Weiler, M., 2017. Snow redistribution for the hydrological modeling of Alpine catchments. *WIREs Water* 4 (5), e1232. <https://doi.org/10.1002/wat2.1232>.
- Garvelmann, J., et al., 2017. Quantification and characterization of the dynamics of spring and stream water systems in the Berchtesgaden Alps with a long-term stable isotope dataset. *Environ. Earth Sci.* 76 (22). <https://doi.org/10.1007/s12665-017-7107-6>.
- Geotest, AG. 1963. Bericht über die seismischen Messungen auf l'Ar du Tsan in Val de Réchy.

- Glas, R., et al., 2019. Hydrogeology of an Alpine talus aquifer: Cordillera Blanca, Peru. *Hydrogeol. J.* 27 (6), 2137–2154. <https://doi.org/10.1007/s10040-019-01982-5>.
- Godsey, S.E., Kirchner, J.W., Tague, C.L., 2014. Effects of changes in winter snowpacks on summer low flows: case studies in the Sierra Nevada, California, USA. *Hydrol. Process.* 28 (19), 5048–5064. <https://doi.org/10.1002/hyp.9943>.
- Griessinger, N., et al., 2019. Implications of observation-enhanced energy-balance snowmelt simulations for runoff modeling of Alpine catchments. *Adv. Water Resour.* 133, 103410. <https://doi.org/10.1016/j.advwatres.2019.103410>.
- Harpold, A.A., Brooks, P.D., 2018. Humidity determines snowpack ablation under a warming climate. *Proc. Natl. Acad. Sci. U.S.A.* 115 (6), 1215–1220. <https://doi.org/10.1073/pnas.1716789115>.
- Hayashi, M., 2020. Alpine hydrogeology: the critical role of groundwater in sourcing the headwaters of the world. *Groundwater*. <https://doi.org/10.1111/gwat.12965>.
- Hood, J.L., Roy, J.W., Hayashi, M., 2006. Importance of groundwater in the water balance of an Alpine headwater lake. *Geophys. Res. Lett.* 33 (13). <https://doi.org/10.1029/2006gl026611>.
- Huth, A.K., Leydecker, A., Sickman, J.O., Bales, R.C., 2004. A two-component hydrograph separation for three high-elevation catchments in the Sierra Nevada, California. *Hydrol. Process.* 18 (9), 1721–1733. <https://doi.org/10.1002/hyp.1414>.
- Jenicek, M., Seibert, J., Staudinger, M., 2018. Modeling of future changes in seasonal snowpack and impacts on summer low flows in alpine catchments. *Water Resour. Res.* 54 (1), 538–556. <https://doi.org/10.1002/2017wr021648>.
- Jenicek, M., Seibert, J., Zappa, M., Staudinger, M., Jonas, T., 2016. Importance of maximum snow accumulation for summer low flows in humid catchments. *Hydrol. Earth Syst. Sci.* 20 (2), 859–874. <https://doi.org/10.5194/hess-20-859-2016>.
- Jodar, J., et al., 2017. Groundwater discharge in high-mountain watersheds: a valuable resource for downstream semi-arid zones. The case of the Berchules River in Sierra Nevada (Southern Spain). *Sci. Total Environ.* 593–594, 760–772. <https://doi.org/10.1016/j.scitotenv.2017.03.190>.
- Jodar, J., et al., 2016. Vertical variation in the amplitude of the seasonal isotopic content of rainfall as a tool to jointly estimate the groundwater recharge zone and transit times in the Ordesa and Monte Perdido National Park aquifer system, north-eastern Spain. *Sci. Total Environ.* 573, 505–517. <https://doi.org/10.1016/j.scitotenv.2016.08.117>.
- Laaha, G., et al., 2016. A three-pillar approach to assessing climate impacts on low flows. *Hydrol. Earth Syst. Sci.* 20 (9), 3967–3985. <https://doi.org/10.5194/hess-20-3967-2016>.
- Langston, G., Bentley, L.R., Hayashi, M., McClymont, A., Pidlisecky, A., 2011. Internal structure and hydrological functions of an alpine proglacial moraine. *Hydrol. Process.* <https://doi.org/10.1002/hyp.8144>.
- Lauber, U., Kotyla, P., Morche, D., Goldscheider, N., 2014. Hydrogeology of an Alpine rockfall aquifer system and its role in flood attenuation and maintaining baseflow. *Hydrol. Earth Syst. Sci.* 18 (11), 4437–4452. <https://doi.org/10.5194/hess-18-4437-2014>.
- Li, D., Wrzesien, M.L., Durand, M., Adam, J., Lettenmaier, D.P., 2017. How much runoff originates as snow in the western United States, and how will that change in the future? *Geophys. Res. Lett.* 44 (12), 6163–6172. <https://doi.org/10.1002/2017gl073551>.
- Li, H., Xu, C.Y., Beldring, S., 2015. How much can we gain with increasing model complexity with the same model concepts? *J. Hydrol.* 527, 858–871. <https://doi.org/10.1016/j.jhydrol.2015.05.044>.
- Lindström, G., Johansson, B., Persson, M., Gardelin, M., Bergström, S., 1997. Development and test of the distributed HBV-96 hydrological model. *J. Hydrol.* 201 (1), 272–288. [https://doi.org/10.1016/S0022-1694\(97\)00041-3](https://doi.org/10.1016/S0022-1694(97)00041-3).
- Liu, F., Williams, M.W., Caine, N., 2004. Source waters and flow paths in an Alpine catchment, Colorado Front Range, United States. *Water Resour. Res.* 40 (9). <https://doi.org/10.1029/2004wr003076>.
- Marty, C., Tilg, A.-M., Jonas, T., 2017. Recent evidence of large-scale receding snow water equivalents in the European alps. *J. Hydrometeorol.* 18 (4), 1021–1031. <https://doi.org/10.1175/jhm-d-16-0188.1>.
- Muir, D.L., Hayashi, M., McClymont, A.F., 2011. Hydrological storage and transmission characteristics of an alpine talus. *Hydrol. Process.* <https://doi.org/10.1002/hyp.8060>.
- Musselman, K.N., Clark, M.P., Liu, C., Ikeda, K., Rasmussen, R., 2017. Slower snowmelt in a warmer world. *Nat. Clim. Change* 7 (3), 214–219. <https://doi.org/10.1038/nclimate3225>.
- Nash, J.E., Sutcliffe, J.V., 1970. River flow forecasting through conceptual model. Part 1—a discussion of principles. *J. Hydrol.* 10, 282–290.
- OFEV 2020. www.hydrodaten.admin.ch.
- Oudin, L., et al., 2005. Which potential evapotranspiration input for a lumped rainfall-runoff model? *J. Hydrol.* 303 (1–4), 290–306. <https://doi.org/10.1016/j.jhydrol.2004.08.026>.
- Pavlovskii, I., Hayashi, M., Itenfisu, D., 2019. Midwinter melts in the Canadian prairies: energy balance and hydrological effects. *Hydrol. Earth Syst. Sci.* 23 (4), 1867–1883. <https://doi.org/10.5194/hess-23-1867-2019>.
- Paznekas, A., Hayashi, M., 2015. Groundwater contribution to winter streamflow in the Canadian Rockies. *Canad. Water Resour. J. / Revue canadienne des ressources hydriques* 41 (4), 484–499. <https://doi.org/10.1080/07011784.2015.1060870>.
- Rohrer, M., Salzmann, N., Stoffel, M., Kulkarni, A.V., 2013. Missing (in-situ) snow cover data hampers climate change and runoff studies in the Greater Himalayas. *Sci. Total Environ.* 468–469 (Suppl), S60–S70. <https://doi.org/10.1016/j.scitotenv.2013.09.056>.
- Santos, A.C., Portela, M.M., Rinaldo, A., Schaeffli, B., 2017. Inference of analytical flow duration curves in Swiss Alpine environments. *Hydrol. Earth Syst. Sci. Discuss.* 1–22. <https://doi.org/10.5194/hess-2017-349>.
- Schaeffli, B., Gupta, H.V., 2007. Do Nash values have value? *Hydrol. Process.* 21 (15), 2075–2080. <https://doi.org/10.1002/hyp.6825>.
- Seibert, J., 1997. Estimation of parameter uncertainty in the HBV model: paper presented at the nordic hydrological conference (Akureyri, Iceland - August 1996). *Hydrol. Res.* 28 (4–5), 247–262. <https://doi.org/10.2166/nh.1998.15>.
- Seibert, J., 2000. Multi-criteria calibration of a conceptual runoff model using a genetic algorithm. *Hydrol. Earth Syst. Sci.* 4 (2), 215–224. <https://doi.org/10.5194/hess-4-215-2000>.
- Seibert, J., Vis, M.J.P., 2012. Teaching hydrological modeling with a user-friendly catchment-runoff-model software package. *Hydrol. Earth Syst. Sci.* 16 (9), 3315–3325. <https://doi.org/10.5194/hess-16-3315-2012>.
- Staudinger, M., Seibert, J., 2014. Predictability of low flow – an assessment with simulation experiments. *J. Hydrol.* 519, 1383–1393. <https://doi.org/10.1016/j.jhydrol.2014.08.061>.
- Staudinger, M., et al., 2017. Catchment water storage variation with elevation. *Hydrol. Process.* 31 (11), 2000–2015. <https://doi.org/10.1002/hyp.11158>.
- Staudinger, M., Weiler, M., Seibert, J., 2015. Quantifying sensitivity to droughts – an experimental modeling approach. *Hydrol. Earth Syst. Sci.* 19 (3), 1371–1384. <https://doi.org/10.5194/hess-19-1371-2015>.
- Spencer, S.A., Silins, U., Anderson, A.E., 2019. Precipitation-Runoff and storage dynamics in watersheds underlain by till and permeable bedrock in Alberta's Rocky Mountains. *Water Resour. Res.* 55. <https://doi.org/10.1029/2019WR025313>.
- SwissTopo, 2008. Vector25 – The Digital Landscape Model of Switzerland. Wabern, Switzerland.
- SwissTopo, 2018. Geocover GA25 1:25'000 - Geological vector datasets for better subsurface management.
- Tague, C., Grant, G.E., 2009. Groundwater dynamics mediate low-flow response to global warming in snow-dominated Alpine regions. *Water Resour. Res.* 45 (7). <https://doi.org/10.1029/2008wr007179>.
- Teutschbein, C., Grabs, T., Karlsen, R.H., Laudon, H., Bishop, K., 2015. Hydrological response to changing climate conditions: spatial streamflow variability in the boreal region. *Water Resour. Res.* 51 (12), 9425–9446. <https://doi.org/10.1002/2015wr017337>.
- Thornton, J., Mariethoz, G., Brunner, P., 2018. A 3D geological model of a structurally complex Alpine region as a basis for interdisciplinary research. *Sci. Data* 5, 180238. <https://doi.org/10.1038/sdata.2018.238>.
- Van Loon, A.F., et al., 2015. Hydrological drought types in cold climates: quantitative analysis of causing factors and qualitative survey of impacts. *Hydrol. Earth Syst. Sci.* 19 (4), 1993–2016. <https://doi.org/10.5194/hess-19-1993-2015>.
- Vincent, A., Violette, S., Áðalgeirsdóttir, G., 2019. Groundwater in catchments headed by temperate glaciers: a review. *Earth Sci. Rev.* 188, 59–76. <https://doi.org/10.1016/j.earscirev.2018.10.017>.
- Viviroli, D., Dürr, H.H., Messerli, B., Meybeck, M., Weingartner, R., 2007. Mountains of the world, water towers for humanity: typology, mapping, and global significance. *Water Resour. Res.* 43 (7). <https://doi.org/10.1029/2006wr005653>.
- Winstral, A., Magnusson, J., Schirmer, M., Jonas, T., 2019. The bias-detecting ensemble: a new and efficient technique for dynamically incorporating observations into physics-based multilayer snow models. *Water Resour. Res.* 55 (1), 613–631. <https://doi.org/10.1029/2018wr024521>.
- Wirth, S.B., Carlier, C., Cochand, F., Hunkeler, D., Brunner, P., 2020. Lithological and tectonic control on groundwater contribution to stream discharge during low-flow conditions. *Water* 12, 821.
- Zhang, D., Cong, Z., Ni, G., Yang, D., Hu, S., 2015. Effects of snow ratio on annual runoff within the Budyko framework. *Hydrol. Earth Syst. Sci.* 19 (4), 1977–1992. <https://doi.org/10.5194/hess-19-1977-2015>.
- Zuecco, G., et al., 2018. Understanding hydrological processes in glacierized catchments: evidence and implications of highly-variable isotopic and electrical conductivity data. *Hydrol. Process.* <https://doi.org/10.1002/hyp.13366>.